

**SURFACE MODIFYING SUPERPARAMAGNETIC IRON OXIDE  
NANOPARTICLES WITH VCAM-1 SPECIFIC PEPTIDE FOR  
ATHEROSCLEROSIS PLAQUE IMAGING**

A Thesis

Presented to:

Supervisor/Reader: Gang Bao, PhD

Co-supervisor: Nazanin Masoodzadehgan, PhD Candidate

Reader: Johnna Temenoff, PhD

**By:**

**Needa Virani**

In Partial Fulfillment

of the Requirements for the Degree

of Bachelor of Science in the

School of Biomedical Engineering

Georgia Institute of Technology

May 2013

COPYRIGHT 2013 BY NEEDA VIRANI

**SURFACE MODIFYING SUPERPARAMAGNETIC IRON OXIDE  
NANOPARTICLES WITH VCAM-1 SPECIFIC PEPTIDE FOR  
ATHEROSCLEROSIS PLAQUE IMAGING**

Approved by:

Dr. Gang Bao, Advisor  
School of Biomedical Engineering  
*Georgia Institute of Technology*

Dr. Johnna Temenoff, Reader  
School of Biomedical Engineering  
*Georgia Institute of Technology*

Nazanin Masoodzadehgan, PhD Candidate  
School of Biomedical Engineering  
*Georgia Institute of Technology*

Date Approved: May 3, 2013

## **ACKNOWLEDGEMENTS**

This publication/project has been funded in whole or in part with the Federal funds from the National Heart, Lung, and Blood Institute, National Institutes of Health, Department of Health and Human Services, under Contract No. HHSN268201000043C. A special thanks to Dr. Gang Bao and Dr. Johnna Temenoff at the Georgia Institute of Technology for reviewing this thesis. A special thanks also to my mentor and PhD candidate Nazanin Masoodzadehgan for helping me design and conduct the proposed project.

## TABLE OF CONTENTS

	Page
ACKNOWLEDGEMENTS	vi
LIST OF FIGURES	viii
LIST OF SYMBOLS AND ABBREVIATIONS	ix
SUMMARY	x
<u>CHAPTER</u>	
1 INTRODUCTION	1
BACKGROUND AND HISTORY	1
JUSTIFICATION OF PROBLEM	4
2 LITERATURE REVIEW	6
3 MATERIALS & EXPERIMENTAL DESIGN	9
4 RESULTS	13
5 DISCUSSION	19
DISCUSSION	19
CONCLUSION	20
REFERENCES	21

## LIST OF FIGURES

	Page
Figure 1: Development of Atherosclerosis	2
Figure 2: Consequences of Plaque Rupture	3
Figure 3: VCAM-1 specific peptide versus antibody affinity	7
Figure 4: Confirmation of VCAM-1 Peptide Surface Modification of 10% PEG- maleimide SPIOs via ILISA Trial 1	14
Figure 5: Confirmation of VCAM-1 Peptide Surface Modification of 10% PEG- maleimide SPIOs via ILISA Trial 2	15
Figure 6: Targeting Study	16
Figure 7: Normalized Fluorescence Intensity of DiI coated SPIOs Trial 1	17
Figure 8: Normalized Fluorescence Intensity of DiI coated SPIOs Trial 2	18

## LIST OF SYMBOLS AND ABBREVIATIONS

SPIOs	Superparamagnetic Iron Oxide Nanoparticles
VCAM-1	Vascular Cell Adhesion Molecule-1
HDL	High-Density Lipoproteins
CRP	C-reactive Protein
IVUS	Intravascular Ultrasound
CT	Computed Tomography
MRI	Magnetic Resonance Imaging
PET	Positron Emission Tomography
FDG	<sup>18</sup> F-Fluorodeoxyglucose
VCAM-NPs	Surface Modified Plaque Specific Antibody Nanoparticles
HUVEC	Human Umbilical Vein Endothelial Cells

## SUMMARY

This study aims to conduct an *in vitro* study confirming the affinity of vascular cell adhesion molecule-1 (VCAM-1) specific peptide surface modified superparamagnetic iron oxide nanoparticles (SPIOs) for atherosclerosis plaque imaging. Currently, plaque detection technology is not as advanced as it could be to detect early onset of atherosclerosis. A novel method is to use biocompatible nanoparticles attracted to the specific sites of interest to image and remove the plaque before further damage. This *in vitro* can be translated into an *in vivo* model making it applicable in future targeting studies for atherosclerosis imaging via PET scans.

# CHAPTER 1

## INTRODUCTION

### BACKGROUND AND HISTORY

Arthrosclerosis is a progressive, inflammatory disorder characterized by lesions or fatty streaks that develop into plaque deposits with a high risk of rupture and thrombosis. Atherosclerosis was initially identified in Egyptian mummies from 1500 BC. Until recently, the development of these plaque streaks has been a mystery.<sup>1,4,5</sup>

Atherosclerosis is considered a gradual, insidious process caused by a combination of endothelial cell dysfunction, lipid oxidation, and lipid accumulation. Endothelial cell dysfunction occurs as cells are exposed to atherogenic milieu such as tobacco smoke, aging, and obesity. When the endothelial cells are damaged, adhesion molecules such as vascular cell adhesion molecule-1 (VCAM-1), and selectins, such as P-selectin, are attracted to the site of injury and function as cell receptors. They signal the binding, rolling, and stable arrest of white blood cells such as monocytes and T-lymphocytes, causing inflammation.<sup>1,4-6</sup>

Atherosclerosis is notably known as a “gradual” process because the fatty streaks generally begin during early childhood and adolescence. Since developed at a young age, these plaques usually go undetected and eventually develop into more insidious, life threatening fat deposits which could instigate myocardial infarction or sudden cardiac death. Figure 1 depicts the development of atherosclerosis starting from the foam cells to the unstable rupture of the plaque.<sup>2,3</sup>



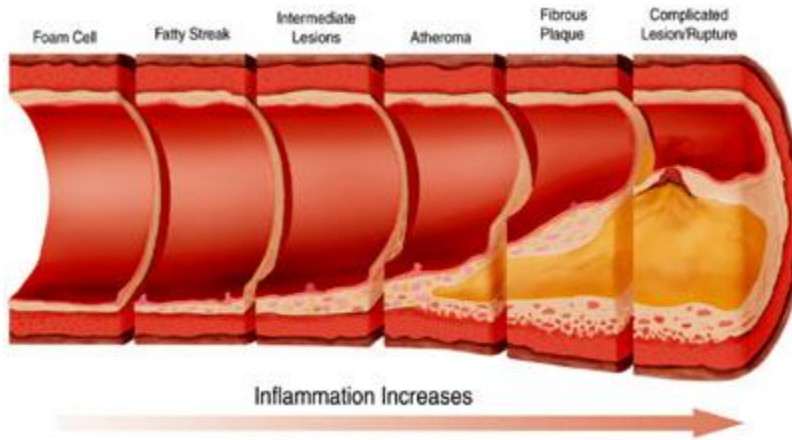


**Figure 1:**  
**Development of Atherosclerosis.**  
 Shows the gradual progression of fatty streak development which progressively grows and becomes more unstable until it finally ruptures.<sup>2</sup>

If caught early on, these plaque deposits are reversible by mobilizing the lesions and removing them from the vessel wall by a process called reverse cholesterol transport which involves a sequence of enzyme-mediated reactions. In general, these enzymes cause the high-density lipoproteins (HDL) to mobilize the fatty deposits so that they can be cleared from the blood stream. If not removed, a stable plaque might grow for decades until it causes stenosis or occlusion, and an unstable plaque will grow vulnerable to spontaneous rupture or thrombosis. This rupture involves the secretion of metalloproteinases, cathepsins, and collagenases by activated macrophages which digest the fibrosis cap and eventually rupture the plaque as seen in Figure 2.<sup>1,3,4,7</sup>

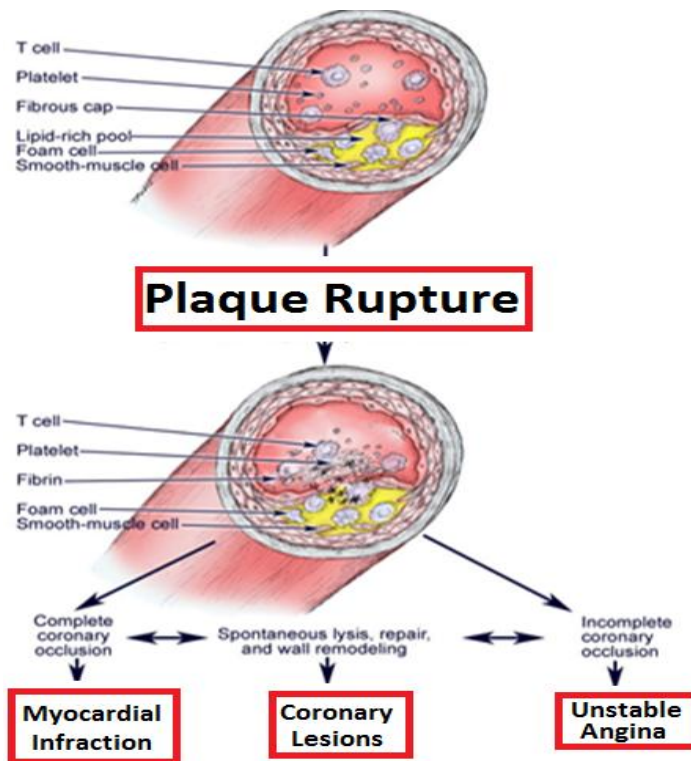


**Figure 2: Consequences of Plaque Rupture.** Depicts the possible consequences of a growing, untreated plaque. It can either remain stable and result in occlusion or become unstable and rupture leading to myocardial infarction, coronary lesions, and unstable anginas.<sup>3</sup>

Current detection techniques, such as serum C-reactive protein (CRP), provide minimal data analysis that limits the assessment of cardiovascular risk. CRP is generally very low in healthy humans, however it significantly increases in patients with atherosclerosis even during early stages of development. Another imaging technique is a contrast angiography that helps to visualize the plaque, however, an angiography is unable to view the entire arterial wall thus eliminating its ability to identify changes in the disease such as alterations in wall thickness and plaque composition or volume. A third prevalent imaging technique is the intravascular ultrasound (IVUS) that compensates for the angiography by allowing the diagnostician to view the progression of the plaque and the effects of drug therapy on the disease, however, it is an invasive procedure. An upcoming technique is computed tomography (CT) which is a minimally invasive procedure that accesses the wall thickening of arteries. Similar to the CT, a high-resolution magnetic resonance imaging (MRI) can also be used as a noninvasive modality

to monitor the plaque development, however both scans are very expensive to conduct on every potential patient.<sup>1,3,4</sup>

Similar to MRI and CT, an additional noninvasive detection method is a positron emission tomography (PET) scan. One contrast agent used is <sup>18</sup>F-fluorodeoxyglucose (FDG), a glucose analog, which is internalized at the site of plaque deposits. The accumulation of FDG can be detected via a PET scan, however, FDG can also be accumulated in any metabolically active cell making PET scans unreliable at times. Using FDGs also results in a high background due to myocardial uptake thus limiting its use for detection. Another contrast agent is <sup>11</sup>C-PK 11195 which specifically binds to activated macrophages as seen at atherosclerosis plaque deposits. PET scans have also been used alongside CT scans to get more reliable results by detecting VCAM-1 or ICAM-1 expression via antibodies or peptides which have a high affinity for the area of interest in *in vitro* and *ex vitro* studies. These antibodies and peptides have been surface modified on SPIOs and microbubbles to attach to plaque deposits for further imaging via PET/CT scans similar to MR imaging.<sup>1-3</sup>

### **JUSTIFICATION OF THE PROBLEM**

About 40% of the adult US population is at immediate risk of developing a cardiovascular disease, such as atherosclerosis, with about 6-20% at risk of developing a coronary disorder within the next ten years. Most studies conducted within the field have focused on later stages of plaque detection. If imaged at a later stage, a plaque can rupture and lead to thrombosis, a heart attack, and even death. This study aims to conduct an *in vitro* study confirming the affinity of VCAM-1 specific peptide surface modified superparamagnetic iron oxide nanoparticles (SPIOs) for early stages of atherosclerosis

plaque imaging. These results can later be translated into further analysis to use VCAM-1 specific peptide surface modified SPIOs *in vivo* for atherosclerosis detection via PET scans.

## CHAPTER 2

### LITERATURE REVIEW

VCAM-1 is present in active endothelial cells, macrophages, and smooth muscle cells (SMCs) and is upregulated in atherosclerosis due to inflammation. It contributes to the recruitment and adhesion of lymphocytes to endothelial cells, forming plaque deposits<sup>1,6</sup>. Currently, there are two developing techniques for detection, antibodies that bind to the surface of VCAM-1 expressing cells and specific peptides that are internalized by VCAM-1 expressing cells. Both methods have been studied extensively *ex vivo* as well as *in vivo* in order to determine which provides the most effective detection mechanism..

VCAM-1 specific antibodies have been used in association with nanoparticles and microbubbles to detect atherosclerosis for MR imaging in previously established *ex vivo* and *in vivo* studies<sup>8,9</sup>. *Ex vivo* studies have shown that anti-VCAM-1 antibodies can be used to detect plaque, however, a low target-to-background ratio makes it difficult to differentiate lesions in *in vivo* mice models<sup>4,10</sup>. This is confirmed by *in vivo* studies conducted on apolipoprotein E<sup>-/-</sup> (apoE<sup>-/-</sup>) mice with surface modified anti-VCAM1 nanoparticles (VCAM-NPs) which were used to detect atherosclerosis lesions via noninvasive MR imaging, however, at 1 hour most VCAM-NPs were still in circulation without clear signs of lesion receptor cell labeling. At 24 hours, accumulation of VCAM-NPs was faintly detected within the lesions. These low intensity signals might have been due to the dissociation of the anti-VCAM1 antibodies from the target caused by the low bond formation rate of the antibodies. In rapid, high-shear circulation through vessels, contact time might not be adequate for antibody attachment to lesions<sup>4,11</sup>. In order to

intensify these signals and improve the target-to-background ratio, a new approach was taken, cell internalization of VCAM-1 specific peptides.

A key advantage of VCAM-1 specific peptides is their capability to amplify signals through cellular internalization which improves uptake >12-fold in comparison to anti-VCAM-1 antibodies (Figure 3)<sup>1,12</sup>. *Ex vivo* studies have been conducted with VCAM-1 specific peptide sequence surface modified nanoparticles (VNPs) in order to determine the specificity of the particle for atherosclerosis lesions in endothelial cells. An 11-fold higher accumulation was seen in activated endothelial cells compared to other VCAM-1 expressing cells such as macrophages, thus suggesting that VNPs can be used to specifically target and detect atherosclerosis<sup>1,6</sup>. Similar to the VCAM-NPs mice model, an *in vivo* study was conducted on apoE<sup>-/-</sup> mice via MRI to determine detection of lesions via peptide internalization. A change in signal intensity of MRI readings was detected with the accumulation of VNPs at atherosclerosis regions which remained detectable for at least 24 hours<sup>1,6,7,13</sup>. This confirms that VNPs provide a more intensified detection of activated endothelial cells in comparison with VCAM-NPs in an *in vivo* model.

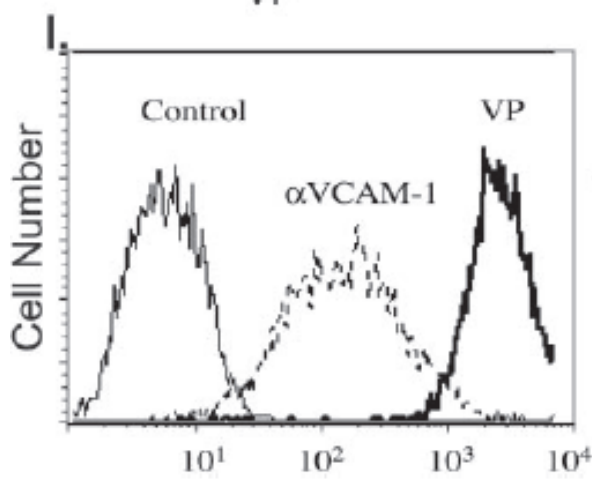


**Figure 3: VCAM-1 specific peptide versus antibody affinity.** Murine cardiac endothelial cells (MCECs) incubated with equimolar concentrations of anti-VCAM-FITC or VCAM-1 peptide (CVHSPNKKCGGSK(FITC)GK) for 2 hours at 37°C. Fluorescence detected via flow cytometry to compare uptake of peptide versus antibody for cells with overexpression of VCAM-1. A 12.1-fold higher fluorescence detected for the peptide (VP) than the antibody (αVCAM-1) incubated cells<sup>1</sup>.

VCAM-1 specific peptide sequences have also been used in *ex vivo* studies conducted on human carotid atheroma cells with a linear derivative of the cyclic peptide sequence used in Kelly et. al (VINP-28). This study suggests that VCAM-1 specific peptide sequences can be used in the future to detect atherosclerosis in a clinical setting for humans <sup>1,6</sup>. VINP-28 can also be used to track the success of the atherosclerosis treatment by detecting reductions in VCAM-1 expression as seen in apoE<sup>-/-</sup> mice with an atherogenic diet that were statin-treated to reduce plaque buildup in vessel walls <sup>6</sup>. This noninvasive, progression methodology can be applied to a human model to track and analyze plaque development or depletion throughout the course of the disease.

Both techniques for atherosclerosis detection have proven effective in *ex vivo* models, however, the long term goal is to transfer this detection method from cell lines and animal models to a human compatible model. VCAM-1 specific cell internalizing peptides have proved to be the better prospective for transitioning due to its higher target-to-background ratio in mice models as well as its ability to remain detectable for longer periods of time. The VCAM-1 specific peptide sequences have also been successfully tested in an *ex vivo* human cell model which broadens the possibility for this to be applied *in vivo* for humans as well as opens up its applicability to help detect other diseases with their respective specified peptide sequences.

## CHAPTER 3

### MATERIALS & EXPERIMENTAL DESIGN

#### *Materials.*

Sodium hydroxide (NaOH), ammonium acetate (AA), hydroxylamine hydrochloride (HH), Tween 20, phosphate buffered saline (PBS), and bovine serum albumin (BSA) were purchased from Sigma. 1,2-distearoyl-sn-glycero-3-phosphoethanolamine-N-[methoxy (polyethylene glycol)-X] (DSPE-PEG(2000)Methoxy) and 1,2-distearoyl-sn-glycero-3-phosphoethanolamine-N-[maleimide(polyethylene glycol)-2000] (DSPE-PEG(2000)Maleimide) were purchased from Avanti. Hydrochloride (HCl) was purchased from VWR. VCAM-1 specific peptide (VINP) was purchased from Genescript. mVCAM/Fc Chimera antigen was purchased from R&D systems. All chemicals were used without further modification.

#### *Experimental Design*

##### *Surface coating and functionalizing SPIOs.*

The SPIOs were functionalized with maleimide groups. The SPIOs were made water soluble via a dual solvent exchange method. Initially, DSPE-PEG(2000)Methoxy and DSPE-PEG(2000)Maleimide were dissolved in water to a final concentration of 10 mg/mL. SPIOs and DSPE-PEG(2000) (90% Methoxy and 10% Maleimide) were mixed at a 1:4 weight ratio. Approximately, 100  $\mu$ L of chloroform was added to the solution. Finally, DMSO was gradually added at 4 times the volume of the contents of the flask. The mixture was left to react for 1 hour before evaporating 20% of the DMSO via a vacuum pump. The entire reaction took place in a dry box.



After the first solvent exchange, the SPIOs were made water soluble by gradually mixing the SPIO solution with water at a 1:5 volume ratio. The solution was filtered to remove the empty micelles via 3 rounds of centrifuge (100K Da cutoff size filters) at 1,500 rcf for 15 minutes and 3 rounds of ultracentrifuge at 75,000 rcf for 30 minutes, both at 4°C. The SPIOs were then filtered with a 25mm syringe-filter to remove any aggregates.

*Size determination by Dynamic Light Scattering (DLS).*

The diameter of the SPIOs was determined via dynamic light scattering (NICOMP Particle Sizing Systems, Santa Barbara, CA). The SPIO solution was diluted with Millipore water (mH<sub>2</sub>O) and size distribution data was collected for 30 minutes. Number-weighted NICOMP analysis was used to calculate the size distribution.

*Iron measurement by Ferrozine Assay.*

The iron content of the SPIOs was determined by mixing 50 µL of dilute SPIO solution with 50 µL of 12M HCl for 30 minutes at room temperature on a shaker. Next, the solution was mixed with 240 µL of 2M NaOH, 50 µL of 4N ammonium acetate, and 110 µL of 5% hydroxylamine HCl for 30 minutes. After incubation, 50 µL of sample was mixed with 50 µL of 0.1% ferrozine solution and incubated for 15 minutes. Absorbance was read at 562 nm with 810 nm as reference.

*VCAM-1 specific peptide conjugation.*

After the SPIOs were filtered and quantified, VCAM-1 specific peptide was added at a 1:20 weight ratio (SPIO:peptide). The reaction was left at 4°C overnight and then centrifuged 3 times at 1,500 rcf for 15 minutes at 4°C. A DLS was conducted to

determine the change in particle size dispersion and a ferrozine assay was run to determine the new iron concentration.

*SPIO-peptide surface modification confirmation (ILISA).*

An ILISA was conducted to confirm VCAM-1 specific peptide surface modification of the SPIOs. ILSA plates were coated with 100  $\mu$ L of 4  $\mu$ g/mL mVCAM/Fc Chimera antigen overnight on a shaker at 4°C. The plates were washed with wash buffer (0.05% Tween 20 in 1X Sigma PBS) three times. The plate was then blocked with 200  $\mu$ L of 1X BSA in PBS and incubated overnight on a shaker at 4°C. The next day, the wells were washed 3 times and 100  $\mu$ L of SPIOs (0 – 100  $\mu$ g/mL) were added to each well. The wells were incubated for 1 hour on a shaker at room temperature. The wells were washed again and 50  $\mu$ L of 6M HCl was added to burn the adhered SPIOs. After 15 minutes, 70  $\mu$ L of 4M NaOH and 80  $\mu$ L of ILISA color (1.5mL 7.5N ammonium acetate, 2.5M of 5% hydroxylamine HCl, and 4mL of 0.1% ferrozine color) were added to each well and absorbance was read at 562 nm with 810 nm as reference.

*Confirming SPIO surface modification and in vitro affinity.*

The peptide-SPIOs were filtered via centrifuge, and DiI was added to a final concentration of 5 $\mu$ g/mL and incubated overnight at 4°C. The SPIOs were filtered with centrifuge and a ferrozine was run again to check the concentration. The human umbilical vein endothelial cells (HUVECs) were split into 5 4-well chambers and incubated for a week until confluent. Lipopolysaccharide (LPS) was added to 9 wells at a final concentration of 100ng/mL and no LPS was added to another 9 wells. The cells were incubated with LPS for 6 hours at 37°C. Next, the cells were washed and the DiI-peptide-

SPIOs were added for 1 hour. The cells were washed and Hoechst and 4% paraformaldehyde were added to stain and fix the cells for DeltaVision imaging.

*Statistical Analysis.*

The images were analyzed with ImageJ. The data gathered from ImageJ was analyzed via ANOVA and one-tailed t-tests.

## CHAPTER 4

### RESULTS

#### *Confirming Surface Modification.*

A DLS was conducted on the SPIOs before and after VCAM-1 peptide conjugation. Before surface modification, the radius of the 10% PEG-maleimide SPIO was 15.89 nm and after the addition of peptide, the radius increased to 20.63 nm. The increase in radius size confirms that there had been some modification to the surface of the SPIOs, however it did not specify what type of modification occurred.

#### *SPIO-peptide surface modification confirmation (ILISA).*

In both trials, the ILISA plates were coated with 4 $\mu$ g/mL of VCAM-1 antigen and blocked with 1% BSA. Unmodified SPIOs was used as a control. In the first trial, concentrations of 0 - 100 $\mu$ g/mL SPIOs were incubated for 1 hour before reading. In general, there was a higher absorbance for the VCAM-1 modified SPIOs. There might have been some contamination for the 0 - 1.56 $\mu$ g/mL wells for the peptide-SPIO sample as seen in Figure 4.

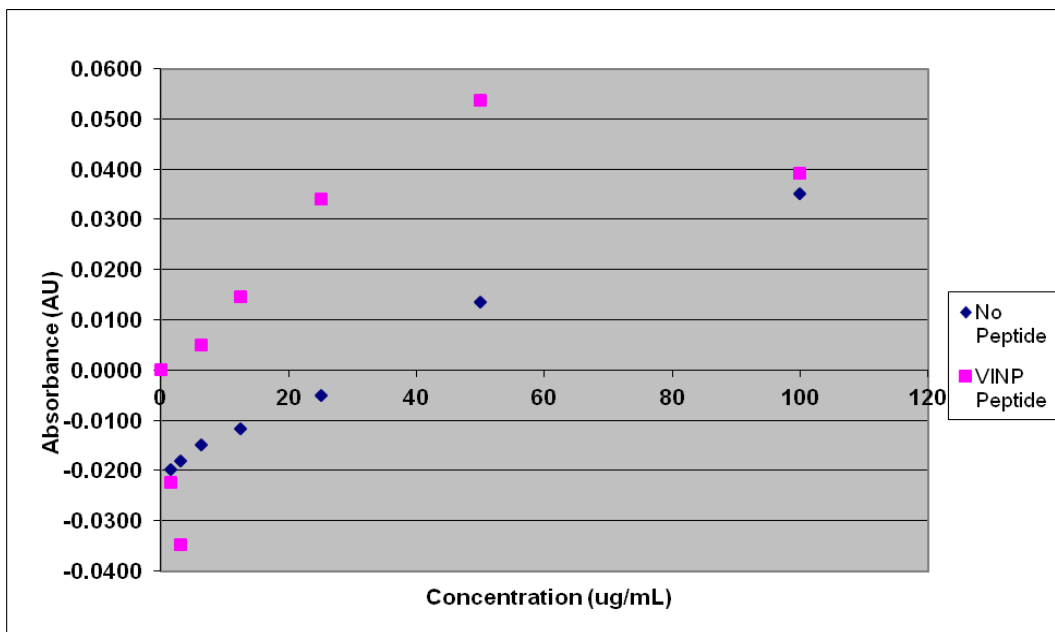


**Figure 4. Confirmation of VCAM-1 Peptide Surface Modification of 10% PEG-maleimide SPIOs via ILISA Trial 1.** Plates were coated with 4ug/mL mVCAM antigen (n=1). 10% PEG-maleimide SPIOs with no peptide was used as control. SPIOs were incubated for 1 hour at room temperature. Concentrations tested were 0 - 100 $\mu$ g/mL. There was a higher absorbance for the peptide coated SPIOs than for the non-surface modified SPIOs.

In the second trial, the same protocol was followed as before however, higher concentrations of SPIOs were used. Concentrations of 0 – 496 $\mu$ g/mL for VCAM-1 peptide surface modified SPIOs and concentrations of 0 - 733 $\mu$ g/mL for the control, unmodified SPIOs were used. Similar to trial 1, Figure 5 shows that the surface modified SPIOs had a higher affinity for VCAM-1 antigen confirming the conjugation.

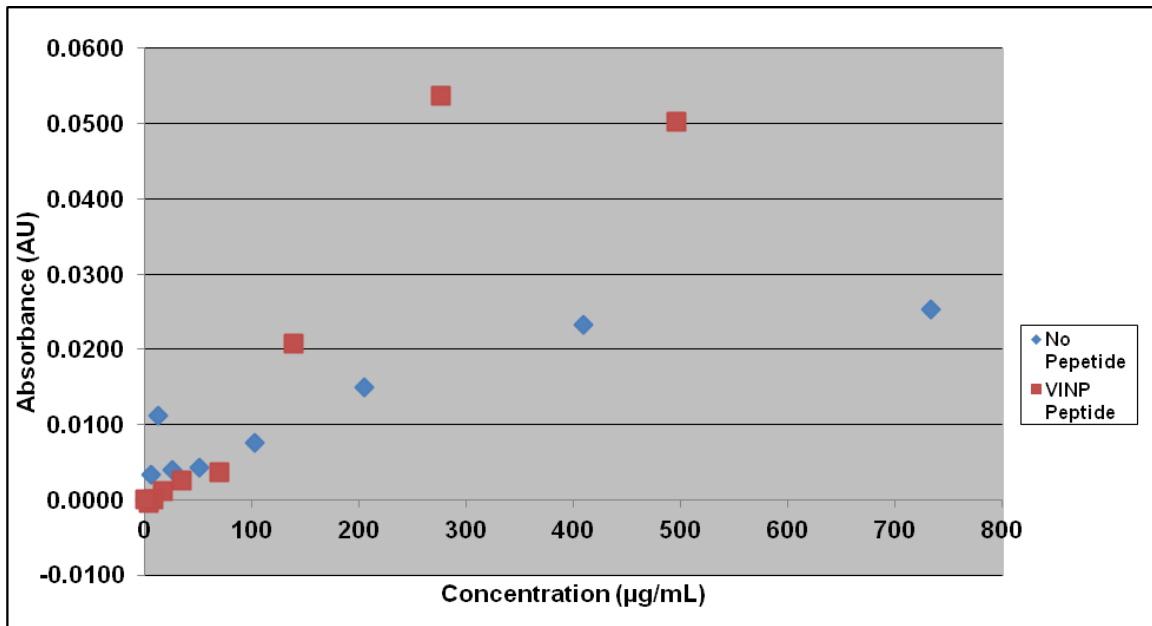


**Figure 5. Confirmation of VCAM-1 Peptide Surface Modification of 10% PEG-maleimide SPIOs via ILISA Trial 2.** Plates were coated with 4ug/mL mVCAM antigen (n=1). 10% PEG-maleimide SPIOs with no peptide was used as control. SPIOs were incubated for 1 hour at room temperature. Concentrations tested were 0 - 496µg/mL for peptide surface modified SPIOs and 0 - 733µg/mL for control SPIOs. There was a higher absorbance for the peptide coated SPIOs than for the non-surface modified SPIOs.

*Confirming SPIO surface modification and in vitro affinity.*

Human umbilical vein endothelial cells (HUVECs) were induced with LPS (100ng/mL) to express VCAM-1 as would be seen in a patient with atherosclerosis. The cells were incubated with surface modified VCAM-1 specific peptide SPIOs, scramble peptide SPIOs, and non-coated SPIOs for 1 hour and imaged via DeltaVision. Through this targeting study, it was determined that more VCAM-1 specific peptide SPIOs were present within cells induced with LPS thus confirming successful surface modification of the SPIOs as seen in Figure 6.

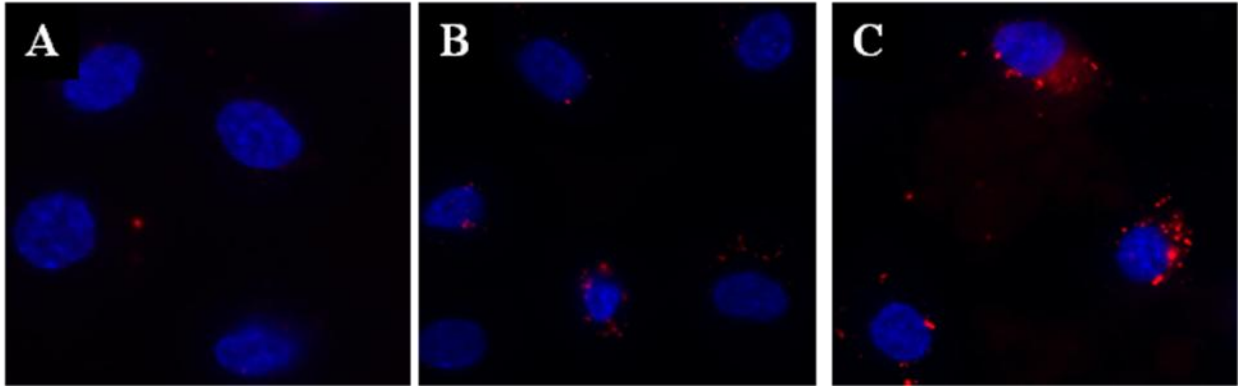


**Figure 6. Targeting Study.** Confirmed that VCAM-1 specific peptide SPIOs (C) have a higher specificity and attraction for LPS induced cells than the control uncoated SPIOs (A) and scramble peptide SPIOs (B). This confirms the surface modification of SPIOs with VCAM-1 specific peptide.

In the first trial, the SPIOs were added at a concentration of 3ug/well for 1 hour. It was seen that most of the SPIOs were internalized by the cells. Non-modified SPIOs and scramble peptide SPIOs were used as controls. The peptide-SPIOs had the highest affinity for LPS induced cells. There was a 3-fold targeting increase from non-modified SPIOs and a 2-fold targeting increase from scramble-SPIOs as seen in Figure 7. It was also seen that there is non-specific binding for non-modified SPIOs and scramble-SPIOs with non-VCAM-1 expressing cells.

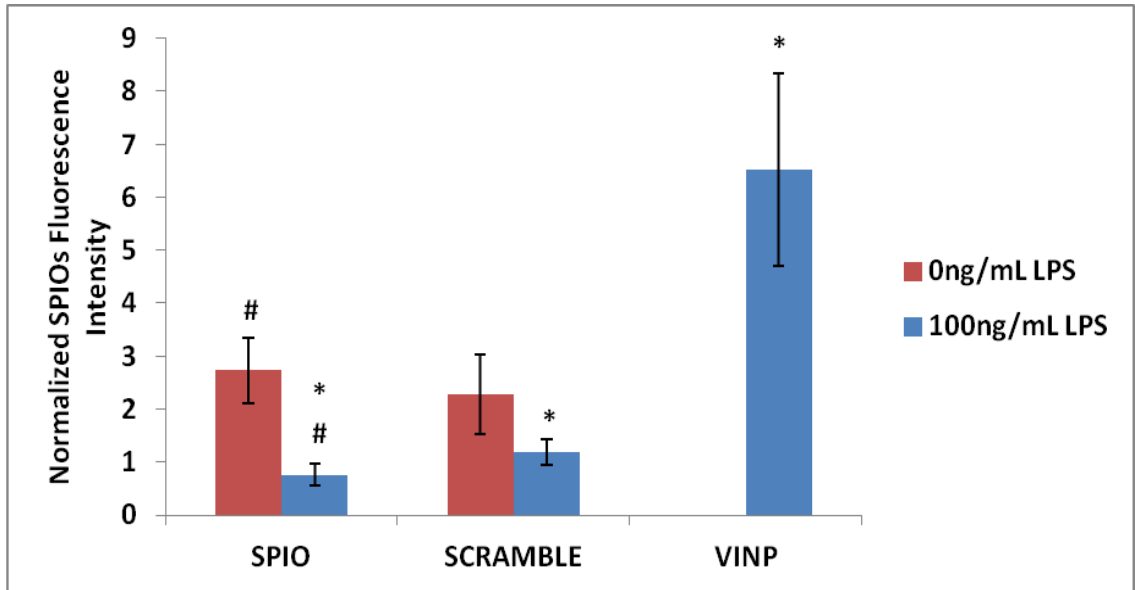


**Figure 7. Normalized Fluorescence Intensity of DiI coated SPIOs Trial 1.** The bar graph shows the average  $\pm$  standard error bars (n=1). The p-values after performing t-tests reaching statistical significance ( $p < .05$ ) are marked on the graph: # indicates a significant difference between 0ng/mL and 100ng/mL LPS induced HUVECs targeting of uncoated SPIOs; \* indicates a significant difference between the VINP coated SPIOs and the uncoated and scramble coated SPIOs for 100ng/mL LPS induced HUVECs.

In the second set of trials, the same protocol was followed. Non-modified SPIOs and scramble peptide SPIOs were used as controls. There was a 7-fold and a 3.5 fold targeting increase from non-modified SPIOs and scramble-SPIOs to peptide-SPIOs, respectively. A 6-fold targeting increase was also seen between 0 and 100ng/mL LPS induced cells which were incubated with peptide-SPIOs as seen in Figure 8.



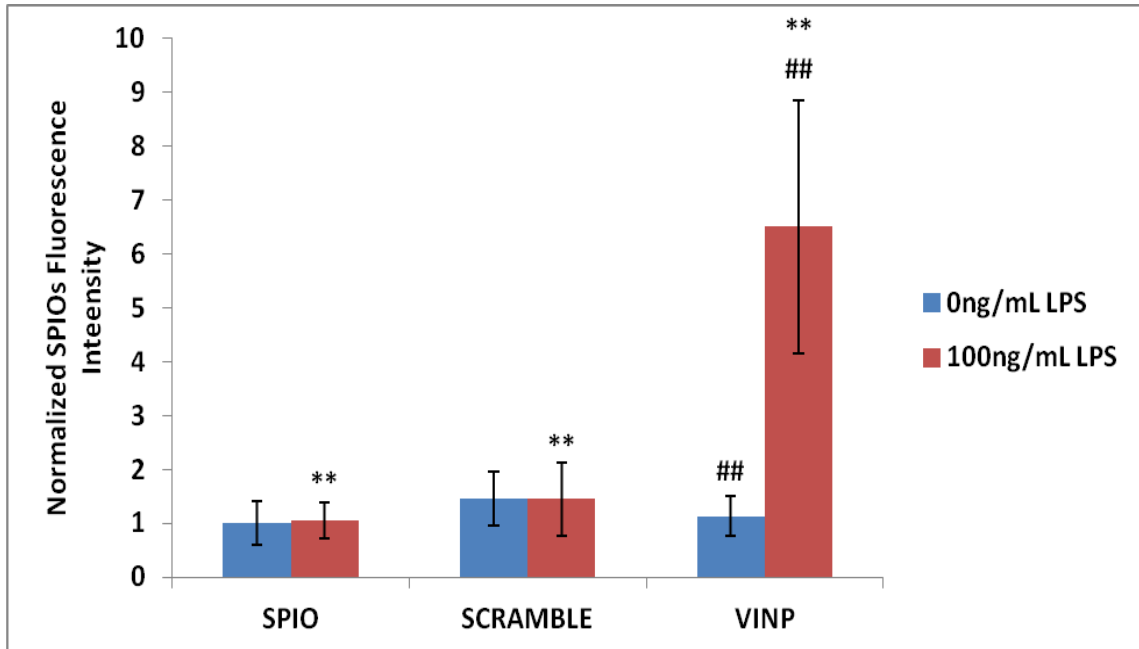


**Figure 8. Normalized Fluorescence Intensity of DiI coated SPIOs Trial 2.** The bar graph shows the average  $\pm$  standard error bars (n=3). The p-values after performing t-tests reaching statistical significance ( $p < .01$ ) are marked on the graph: \* indicates a significant difference between the peptide coated SPIOs and the uncoated and scramble coated SPIOs for 100ng/mL LPS induced HUVECs; # indicates a significant difference between 0 and 100ng/mL LPS induced HUVECs targeting of peptide coated SPIOs.

## CHAPTER 5

### DISCUSSION

The DLS, ILISA, and *in vitro* studies have shown that there is a higher attraction for peptide-SPIOs than non-modified SPIOs and scramble-SPIOs in LPS induced HUVECs representing *in vivo* atherosclerosis plaque cells. In the first trial, only a 3-fold targeting increase from non-modified SPIOs to peptide-SPIOs was seen while in the second trial there was a 7-fold increase. A similar inconsistency is seen between the 2-fold targeting increase from scramble-SPIOs to peptide-SPIOs in the first trial compared to the 3.5-fold increase in the second trial. These inconsistencies might have been due to the sample size used in each trial. In the first trial, not enough product was retrieved to run more than one well per sample. The standard error was determined by averaging the data from three images per well. In the second trial, however three images were taken per well and three wells were used so that the results would be more reliable.

Another possibility for these inconsistencies is that when conducting the ferrozine of previous samples, a discrepancy was noticed between the concentration reading and the concentration of SPIOs added to the sample. The readings for the surface modified SPIOs was significantly lower than the readings for just the SPIOs which could mean that the peptide on the surface is distorting the iron content reading. A similar discrepancy was seen with DiI and non-DiI coated SPIOs. The DiI coated SPIOs had significantly lower concentrations of iron than the non-coated ones. Due to the discrepancies, the amount of iron added to each well might have been different which might also explain why the differences between the VCAM-1 coated and scramble coated SPIOs is smaller than expected from previous studies.<sup>1,6</sup> In either case, there was a significance present

between the VCAM-1 coated SPIOs and the uncoated and scramble coated SPIOs which supports the hypothesis that VCAM-1 specific peptides modified SPIOs have a higher affinity for VCAM-1 expressing cells compared to the controls.

In trial 1, there was also a significant increase in the targeting between the 0 and 100ng/mL LPS treated cells for non-coated SPIOs. Similar to the inconsistencies stated previously, this difference in targeting might have been due to the fact that only one well was imaged since in the second study, the 0 and 100 ng/mL had similar targeting. Similar to the non-coated SPIOs, a 6-fold increase was seen between the 0 and 100ng/mL peptide-SPIOs which was expected since the targeting should have increased when the cells were expressing VCAM-1.

Overall, these studies have shown that there is a significant increase in targeting of VCAM-1 expressing cells due to the surface modification of SPIOs with VCAM-1 specific peptides. This study will need to be repeated to confirm these results with replicates before moving onto further testing and analysis.

## **CONCLUSION**

These studies have shown a strong correlation between peptide-SPIOs and VCAM-1 expressing HUVECs as would be seen in plaque deposits during early development. Once these results are confirmed, this study can progress towards an *ex vivo* and *in vivo* models with atherosclerosis induced mice to test if the SPIOs will have a similar targeting power.

## REFERENCES

1. Kelly KA, Allport JR, Tsourkas A, Shinde-Patil VR, Josephson L, Weissleder R. Detection of vascular adhesion molecule-1 expression using a novel multimodal nanoparticle. *Circ.Res.* Feb 2005;96(3):327-336.
2. Toth PP. Atherosclerosis: The Underlying Disease. *The Journal of Family Practice.* 2009;58(11).
3. Boudi FB, Ahsan CH, III GS, Talavera F, Compton SJ, Subhi Y. Coronary Artery Atherosclerosis. *Medscape Reference-Drugs, Diseases & Procedures.* 2009. <http://emedicine.medscape.com/article/153647-overview#showall>.
4. Kaufmann BA, Sanders JM, Davis C, et al. Molecular imaging of inflammation in atherosclerosis with targeted ultrasound detection of vascular cell adhesion molecule-1. *Circulation.* Jul 2007;116(3):276-284.
5. Nahrendorf M, McCarthy JR, Libby P. Over a Hump for Imaging Atherosclerosis Nanobodies Visualize Vascular Cell Adhesion Molecule-1 in Inflamed Plaque. *Circ.Res.* Mar 2012;110(7):902-903.
6. Nahrendorf M, Jaffer FA, Kelly KA, et al. Noninvasive vascular cell adhesion molecule-1 imaging identifies inflammatory activation of cells in atherosclerosis. *Circulation.* Oct 2006;114(14):1504-1511.
7. Nahrendorf M, Keliher E, Panizzi P, et al. F-18-4V for PET-CT Imaging of VCAM-1 Expression in Atherosclerosis. *JACC-Cardiovasc. Imag.* Oct 2009;2(10):1213-1222.
8. Iiyama K, Hajra L, Iiyama M, et al. Patterns of vascular cell adhesion molecule-1 and intercellular adhesion molecule-1 expression in rabbit and mouse

- atherosclerotic lesions and at sites predisposed to lesion formation. *Circ.Res.* Jul 1999;85(2):199-207.
9. Ferrante EA, Pickard JE, Rychak J, Klibanov A, Ley K. Dual targeting improves microbubble contrast agent adhesion to VCAM-1 and P-selectin under flow. *Journal of Controlled Release.* Dec 2009;140(2):100-107.
  10. Jaffer FA, Libby P, Weissleder R. Molecular and cellular imaging of atherosclerosis - Emerging applications. *Journal of the American College of Cardiology.* Apr 2006;47(7):1328-1338.
  11. Tsourkas A, Shinde-Patil VR, Kelly KA, et al. In vivo imaging of activated endothelium using an anti-VCAM-1 magneto-optical probe. *Bioconjugate Chemistry.* May-Jun 2005;16(3):576-581.
  12. Thorek DLJ, Chen AK, Czupryna J, Tsourkas A. Superparamagnetic Iron Oxide Nanoparticle Probes for Molecular Imaging. *Annals of Biomedical Engineering.* 2006;34(1):23-38.
  13. Southworth R, Kaneda M, Chen JJ, et al. Renal vascular inflammation induced by Western diet in ApoE-null mice quantified by F-19 NMR of VCAM-1 targeted nanobeacons. *Nanomedicine-Nanotechnology Biology and Medicine.* Sep 2009;5(3):359-367.